Hyperbranched poly(benzimidazole-co-benzene) with honeycomb structure as a membrane for high-temperature proton-exchange membrane fuel cells

Sambhu Bhadra[a], Nam Hoon Kim[b], Ji Sun Choi[b], Kyong Yop Rhee[c], Joong Hee Lee[a,b,*]

[a] Dept of Polymer & Nano Engineering, Chonbuk National University, Duckjin-dong 1Ga 664-14, Jeonju, Jeonbuk, 561-756, South Korea
[b] Department of Hydrogen and Fuel Cell Engineering, Chonbuk National University, Duckjin-dong 1Ga 664-14, Jeonju, Jeonbuk, 561-756, South Korea
[c] Department of Mechanical Engineering, Kyung Hee University, Yongin, 446-701, South Korea

ARTICLE INFO

ABSTRACT

Hyperbranched poly(benzimidazole-co-benzene) (PBIB) with a honeycomb structure is synthesized by condensation polymerization of trimesic acid (TMA) and 3,3′-diaminobenzidine (DAB) for use as a membrane high-temperature proton-exchange membrane fuel cells (HT-PEMFCs). The hyperbranched honeycomb structure of polybenzimidazole (PBI) has been introduced to impart higher mechanical strength to doped PBI membranes. The stress at break of the phosphoric acid doped PBI (DPBIB) membrane (29 ± 3 MPa) is comparable with that of Nafion (28 ± 2 MPa) and much superior to doped PBI membranes. The DPBIB membrane exhibits lower proton conductivity than Nafion 115. On the other hand, the proton conductivity of Nafion 115 is enhanced with increase in relative humidity, whereas humidity has only a moderate effect on the proton conductivity of the DPBIB membrane. Consequently, the Nafion 115 membrane in a fuel cell cannot operate in the absence of humidity, whereas the DPBIB membrane can perform well. The power output of the DPBIB membrane in a fuel cell is superior under humid conditions than under dry conditions. The maximum power output from the DPBIB and Nafion 115 membranes is comparable under humid conditions. It is concluded that the DPBIB membrane, but not Nafion, is suitable for application in HT-PEMFCs.

© 2009 Elsevier B.V. All rights reserved.

1. Introduction

Proton-exchange membrane fuel cells (PEMFCs) have attracted increasing attention because of their successful demonstration as power generators in both stationary and transportation applications. A key component of these devices is the membrane–electrode assembly (MEA), which comprises an ion-exchange membrane with catalytic powder electrodes attached to the two membrane faces. The most successful membrane is Nafion, which offers quite good performance below 90 °C under fully hydrated conditions. In addition, it provides good chemical and mechanical stability, high power density, environmentally friendly operation, all-solid construction, and low material corrosion. The proton conductivity of Nafion is, however, strongly dependent on the presence of water. Consequently, the operational temperature is limited to below 100 °C. The gases (typically, hydrogen and oxygen) need to be well humidified before entering the fuel cell. During the operation of a fuel cell, accumulation of excess water at the cathode side causes flooding which prevents oxygen from approaching the catalyst and thereby gives rise to mass-transfer resistance. On the other hand, the starvation of water at the anode side results in a decrease in conductivity. This is called the "issue of water management", which significantly influences the performance of fuel cells. Furthermore, the barrier properties of the membrane are usually insufficient when methanol is used as a fuel, i.e., methanol crossover is large and decreases the cell potential due to the formation of a mixed potential and lower fuel efficiency. The other challenges are the high cost, critical system design and operation with respect to water management, low tolerance of fuel impurities, and poisoning of the electrode catalyst by carbon monoxide [1–5].

To resolve the abovementioned problems, recent research on PEMFC has focused mainly on the development of a high-temperature PEMFC (HT-PEMFC) which operates above 100 °C [6–22]. Such operation ensues higher efficiencies, high power density, reduced sensitivity to carbon monoxide poisoning of the catalyst and better controllability with a simpler system design and operation (because of the absence of water management issues in the membrane). In addition, the barrier properties of these membranes are enhanced because of the single phase morphology of the material [7,10–12]. The polymers used in the preparation of HT-PEMFC membranes contain basic groups that

can form complexes with stable acids, e.g., polybenzimidazole (PBI), poly(pyridine), poly(pyrimidine), polyimidazoles, polybenzthiazoles, polybenzoxazoles, polyoxadiazoles, polyquinoxalines, polythiadiazoles, and poly(tetrazapyrenes) [6–9]. The phosphoric acid doped PBI membrane is the most preferred basic polymer membrane for HT-PEMFCs and can be operated at 100–220 °C [6,9]. PBI-type membranes are doped with an excess of phosphoric acid to increase their proton conductivity. The mechanical strength of PBI-type membranes, however, decreases with an increasing degree of doping [14,16]. This is a severe problem for PBI-type membranes, because good mechanical strength is an indispensable requirement for the membrane to perform in an actual fuel cell. Different strategies are being explored to improve the mechanical strength of doped PBI. These include the introduction of inorganic fillers [12], preparation of polymeric acid–base blend membranes, referred to as ionic cross-linking [17], covalent cross-linking by thermal treatment [18], chemical cross-linking using different cross-linkers, such as 3,4-dichloro-tetrahydro-thiophene-1,1-dioxide [19], p-xylene dichloride [20], p-xylene dibromide [21], dichloromethyl phosphinic acid [22].

The aim of this study is to improve the mechanical strength of PBI-type membranes by introducing a hyperbranched honeycomb structure. A hyperbranched PBI-type polymer with a honeycomb structure is prepared by the condensation polymerization of TMA and DAB for HT-PEMFC. The introduction of a hyperbranched honeycomb structure is expected to impart high mechanical strength even after doping with phosphoric acid and prevail over the very much weakening of PBI-type membranes after doping.

2. Experimental

2.1. Materials

3,3′-Diaminobenzidine (DAB) and trimesic acid (TMA) were purchased from Tokyo Chemical Industry, Co. Ltd., Japan. Polyphosphoric (PPA) acid, calcium chloride and phosphoric acid were obtained from Sigma Aldrich, Germany. Sulfuric acid was acquired from Duksan Pure Chemicals Co. Ltd., Korea. Nafion 115 was procured from Du Pont, USA. The gas-diffusion electrode (GDE), ELAT GDE-LT120EW with a platinum loading of $5\,g\,m^{-2}$ was purchased from E-TEK, Inc., USA.

2.2. Synthesis of poly(benzimidazole-co-benzene) (PBIB)

Depending on the number of reactive sites in each monomer, TMA and DAB were used at a ratio of 2:3 (TMA was 20 mmol or 4.20 g and DAB was 30 mmol or 6.42 g). The monomers were mixed thoroughly and then placed in a 500 mL three-necked flask. 320 g PPA was added. The reaction flask was equipped with a calcium chloride drying tube and a nitrogen inlet. Simultaneous stirring and heating of the mixture were carried out on a magnetic heating/stirring mantle. The mixture was heated to $275 \pm 5\,°C$ for 9 h. Lobato et al. [16] reported that the molecular weight of PBI is increased with increasing reaction temperature and that 275 °C is the optimum temperature for the synthesis of high molecular weight PBI [16]. If the reaction temperature is increased further, PPA will decompose. They also reported that 160 g PPA is the optimum amount for 15 mmol of the monomers and other catalysts, such as triphenyl phosphate, and a drying agent such as P_2O_5, is not essential for carrying out the polymerization reaction [16]. Therefore, the optimum reaction conditions and materials used in this study were those reported by Lobato et al. [16]. A progressive increase in the viscosity of the reaction mixture was observed as the reaction proceeded. After a 9 h reaction, the resulting dark purple reaction mixture was cooled and poured into deionized water in

order to isolate the golden-yellow colour polymer. Subsequently, the polymer was dialyzed against deionized water until a constant pH was reached. The aqueous dispersion was not neutralized with a base in order to avoid possible hydrolysis or de-polymerization reactions. The polymer powder was dried in a vacuum oven at 150 °C for 24 h. Finally, the polymer was ground to obtain a fine gold-brownish PBIB powder. The yield of PBIB was ~90%. The entire synthesis procedure is schematically presented in Fig. 1.

2.3. Film preparation

The PBIB powder is insoluble in all available solvents including 97% H_2SO_4 because of its highly rigid, hyperbranched structure. Therefore, it is quite challenging to cast the PBIB film from its powder form any suitable solvent. The PBIB film was prepared by a hot press method using 97% H_2SO_4 as a binder. 0.5 g of PBIB powder was mixed with 5 mL H_2SO_4 and then placed between two Teflon sheets (15 cm × 15 cm × 0.5 cm). The entire assembly was heated to 230 °C for 40 min under a pressure of 2 in a carver hot press (Model 3721, USA). After the elapsed time, the assembly was allowed to cool to room temperature under pressure. A fine thin film of PBIB was automatically separated out. The film thus obtained was boiled in deionized water for 2 h, and then preserved in cold deionized water until needed. This film was designated UPBIB.

2.4. Doping

The UPBIB films were immersed in a 10 M phosphoric acid solution for 4 weeks. Lobato et al. [23] reported that the immersion of a PBI film in a 10 M H_3PO_4 solution for 2 weeks is sufficient to reach total saturation. In this study, however, the UPBIB films were immersed for 4 weeks in order to ensure total saturation. Afterwards, the membranes were kept in a vacuum oven for 12 h at ambient temperature to evaporate the water. The phosphoric acid doped PBIB film was designated DPBIB.

2.5. Pretreatment of Nafion membrane

Nafion 115 was boiled in 3% H_2O_2 for 1 h, rinsed repeatedly in boiled deionized water, boiled in 0.5 mol l^{-1} H_2SO_4 for 1 h, and then kept in a vacuum oven for 12 h at ambient temperature to evaporate the water [24].

2.6. Characterization

The FT-IR spectrum was recorded on a NICOLET 6700 FT-IR instrument (Thermoscientific, USA). The sample powder was dispersed in KBr powder and compressed into pellets.

The ultra-high resolution microscopic study was accomplished with a field emission transmission electron microscope (FE-TEM), JEM-2200 FS from JEOL, Japan, with an accelerating voltage of 200 keV. The polymer powder (5 wt.%) was dispersed in ethanol and mixed thoroughly. This slurry was used to deposit the polymer thin layer on the FE-TEM sample grid (copper–carbon).

Thermogravimetric analysis (TGA) was carried out using a TGA, Q50 instrument from TA Instruments, USA. The experiment was accomplished under a nitrogen atmosphere over the temperature range of 40–900 °C at a heating rate of 20 °C min^{-1}.

Elemental analysis was performed on an Elementar Analysensysteme GmbH VarioEL V4.01 in CHNS Mode.

The stress at break and the elongation at break of the membranes were measured at room temperature using a universal test machine (LR5K plus model, Lloyd. Co.) at a crosshead speed of 50 mm min^{-1}, according to ASTM D412. Dumbbell-shaped specimens were cut from the membranes for the measurement. An average of five test results is reported.

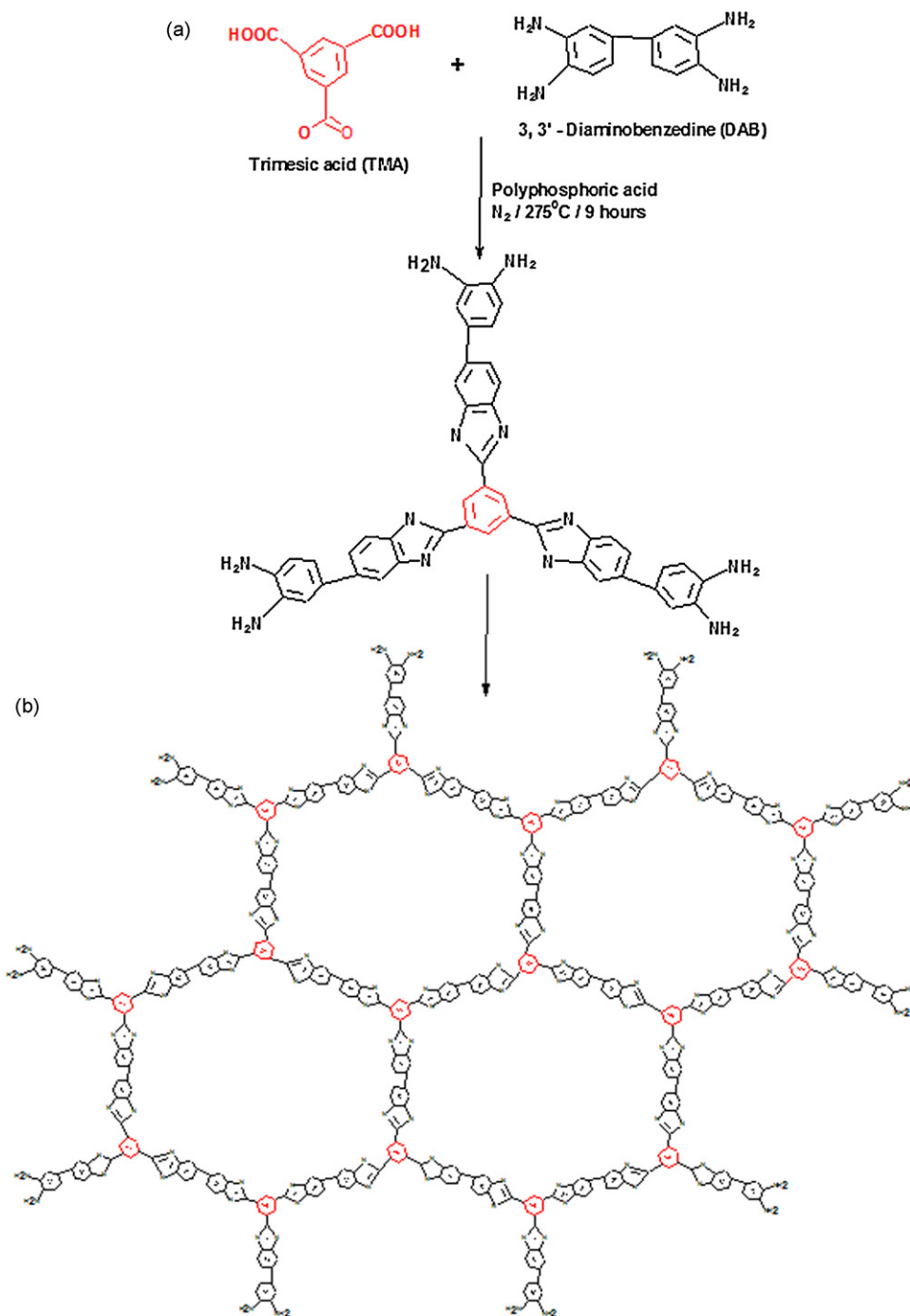**Fig. 1.** Schamatic illustration of synthesis of poly(benzimidazole-co-benzene) (PBIB) by condensation polymerization of 3,3′-diaminobenzedine (DAB) and trimesic acid (TMA).

The proton conductivity of the membranes was measured by the four-probe method using a BekkTech conductivity test cell in conjunction with a PGZ 301 Dynamic EIS Voltammeter. Temperature and humidification were controlled using a Globe Tech Computer Cell GT fuel cell test station. The humidity within the testing chamber was controlled by means of a dew point system that consisted of temperature regulation and a deionized water inlet. The four-point conductivity measurements involved the use of four electrodes which were placed around the cell to obtain the resistance values. Two electrodes were attached to the current-collectors of the test cell and the other two electrodes were attached directly to the platinum sensor wires to measure the potential drop across the membrane. A membrane, approximately 5 cm in length and 2 cm in width, was cut and placed in a BekkTech conductivity test cell. An alternating current (a.c.) was passed through the two outer electrodes and the decrease in sample resistance was recorded from the a.c. potential difference between the two inner electrodes. Pre-installed LabVIEW software controlled the entire system. The proton conductivity was calculated automatically using the following equation.

$$\sigma = \frac{L}{RWT} \tag{1}$$

where σ is the proton conductivity, L is the length (cm) parallel to the ion flow, R is the decrease in resistance (ohm) between the inner electrodes, W is the width (cm), and T is the thickness (cm) of the membrane.

The performance of the pretreated Nafion 115 and DPBIB membranes in a single cell was evaluated by means of the following method. The membrane–electrode assembly (MEA) was prepared by hot pressing two $2\,cm \times 2\,cm$ gas-diffusion electrodes (GDEs), on both sides of the membrane ($5\,cm \times 5\,cm$) keeping the catalyst coated face of the GDE on the membrane side. Hot pressing was carried out for 10 min at 135 °C and a pressure of $100\,kg\,cm^{-2}$. Subsequently, the MEA was mounted in a $5\,cm \times 5\,cm$ fuel cell test fixture that consisted of two flow-field plates and two end-plates. The flow-field plates, with $2\,cm \times 2\,cm$ active area, were made of graphite impregnated with a phenolic resin and had a serpentine geometry with a channel-to-land ratio of 1:1. Two aluminum end-plates with attached heaters were used to clamp the flow-field plates.

The single cell was connected to a fuel cell testing station (FCT-TS 300, Fuel Cell Tech., Inc.). Before testing, the cell was purged with dry nitrogen gas for 30 min at room temperature and then activated for 3 h at a fuel (hydrogen) flow rate of $100\,mL\,min^{-1}$ at the anode and an air flow rate of $400\,mL\,min^{-1}$ at the cathode under dry conditions at 70 °C and under open-circuit condition. The current–voltage characteristics of both membranes under hydrogen and air flow were measured at different temperatures and at different current densities with and without humidity. For 100% humidification, hydrogen and air were fed to the fuel cell through a humidity chamber, and the gases were introduced directly to maintain the dry conditions. The experiments were first carried out under dry conditions and then under 100% humidity conditions.

3. Results and discussion

3.1. FT-IR analysis

The FTIR spectra of the PBIB powder and UPBIB film are shown in Fig. 2. The PBIB powder exhibits strong absorption peaks at 3400, 1626, 1456, 1062, 947, 893, 803, and 491 cm^{-1}. The broad peak at 3400 cm^{-1} is assigned to the N–H asymmetric stretching [25,26]. The peak at 1626 cm^{-1} is due to the C=N/C=C stretching vibration, absorption at 1456 cm^{-1} is ascribed to the in-plane ring vibration of benzimidazole [27]. The absorption peak at 1062 cm^{-1} is due to the stretching vibration of C–N [28,29]. The absorption bands from 900 to 650 cm^{-1} are assigned to aromatic C–H out-of-plane bending vibrations [25]. There is no residual carbonyl absorption
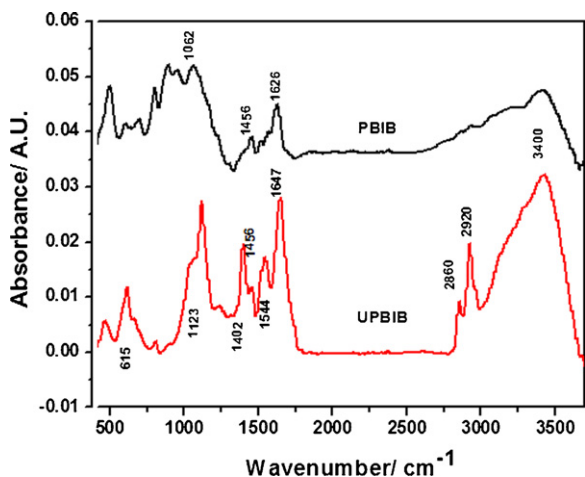
between 1780 and 1650 cm^{-1}, which indicates a complete reaction between TMA and DAB, and the formation of PBIB with the structure presented in Fig. 1.

Compared with the PBIB powder, the UPBIB film exhibits a few extra absorption peaks at 2920, 2860, 1544, 1402, 1123, and 615 cm^{-1}. The bands for O–H and N–H appear in the region from 3700 to 2500 cm^{-1} [25]. Therefore, the extra peaks for the UPBIB film at 2920 and 2860 cm^{-1} may be due to the O–H stretching vibration of the sulfonic acid group. The band at 1626 cm^{-1} for the PBIB powder is blue and shifts to 1647 cm^{-1} in the UPBIB film spectrum with increased intensity and an extra band appears at 1544 cm^{-1}. This suggests the presence of sulfonic acid groups [30]. H_2SO_4 was used as a binder for the PBIB film preparation. In presence of H_2SO_4, PBIB undergoes sulfonation through an electrophilic aromatic substitution reaction. The extra peaks at 1123 and 1402 cm^{-1} in the spectrum of the UPBIB film are typical of the stretching vibration of arylsulfone groups [31,32]. The extra peak at 615 cm^{-1} in the UPBIB spectrum is due to the C–S stretching vibration [33,34].

3.2. Elemental analysis

From elemental analysis of the UPBIB film, the ratio of N:S is found to be 12.6:5.8 (wt.%) or 5:1 (atom ratio). This demonstrates the presence of some sulfonic acid groups in the molecular structure of UPBIB, even though the degree of sulfonation is very low.

3.3. FE-TEM

FE-TEM was used to observe the molecular structure of PBIB, as shown in Fig. 3. The whole TEM image appears like a net that consists of highly ordered and uniform six-membered units. The TEM image confirms the formation of a hyperbranched honeycomb structure, as shown schematically in Fig. 1. One TMA molecule initially reacts with three DAB molecules to form a type of tri-dented legend containing 3×2 open amine groups (Fig. 1a). These amines groups can further react only with TMA monomers during the condensation reaction closing the amine groups with carboxylic acid groups and forming six-membered rings, as shown in Fig. 1(b). The structure of the final polymer is expected to consist of uniform, highly ordered, six-membered rings as also seen in the TEM image (Fig. 3).
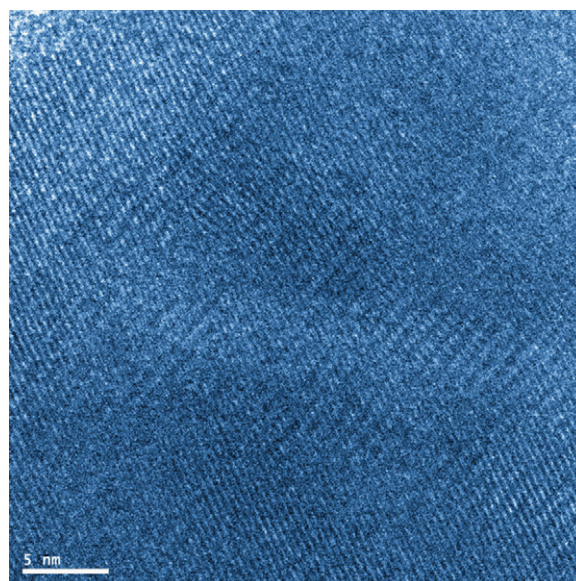

Fig. 2. FT-IR spectra of PBIB powder and UPBIB film.

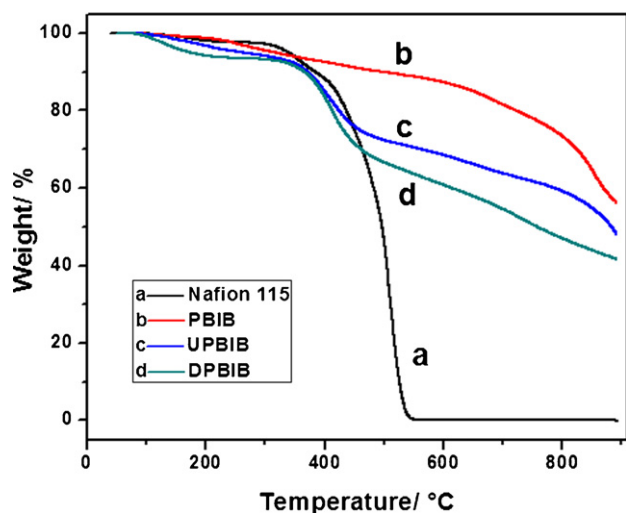**Fig. 3.** Field emission transmission electron microscopic (FE-TEM) image of PBIB.

Fig. 4. TGA plots of (a) Nafion 115, (b) PBIB powder, (c) undoped PBIB film (UPBIB) and (d) phosphoric acid doped PBIB film (DPBIB).

3.4. Thermogravimetric analysis (TGA)

The thermal stability of the polymers was determined by TGA analysis (Fig. 4). The decomposition of the Nafion 115 starts at from 300 °C and is completed before 550 °C. The Nafion 115 undergoes 100% decomposition. By contrast, decomposition of the PBIB powder begins at 250 °C and continues up to the final experimental temperature, viz., 900 °C. The thermal decomposition pattern of the PBIB powder suggests that the PBIB membrane can be used safely up to 220 °C. The doped and undoped PBIB films initially exhibit some weight loss at around 100–250 °C owing to the loss of moisture. The UPBIB film shows more weight loss at approximately 350–450 °C compared with the PBIB powder. This is attributed to decomposition of sulfonic acid groups present in the UPBIB film. The DPBIB film shows further higher weight loss over the same temperature region compared with the UPBIB film. This is due to the decomposition of both the sulfonic acid groups and doped phosphoric acid present in the DPBIB film. The PBIB powder and films do not undergo 100% decomposition, even after heating to 900 °C. Polymers with an aromatic backbone always leave some residue even at 900 °C. The residual materials are mainly thermally stabilized carbonized materials [35,36]. The PBIB powder, UPBIB film and DPBIB film leave approximately 56.2, 48.1 and 41.5 wt.% of residue, respectively, at 900 °C. From the residues at 900 °C, the weight percentage of sulfonation in the UPBIB film and the weight percentage of phosphoric acid, i.e., the degree of doping in the DPBIB film were calculated. The UPBIB and DPBIB films contain approximately 14.4 wt.% of sulfonic acid group with respect to the PBIB powder. These sulfonic acid groups were introduced in the polymer structure during the preparation of films as discussed earlier. The DPBIB film contains 13.7 wt.% of phosphoric acid with respect to the UPBIB film. The uptake of phosphoric acid by the PBI-type membranes is as high as 572 wt.% [36]. The very low uptake of phosphoric acid by the UPBIB film is attributed to the presence of some sulfonic acid groups that act as a dopant and compact the honeycomb structure of the polymer.

3.5. Mechanical properties

The mechanical properties of the Nafion 115, UPBIB and DPBIB films are listed in Table 1. The stress at break of the UPBIB film (33 ± 2 MPa) is much higher than that of Nafion 115 film (28 ± 2 MPa). After doping, however, the stress at break of the DPBIB film is deteriorated to some extent but the value (29 ± 3 MPa) is still

Table 1
Mechanical properties of Nafion 115 and PBIB films.

Sample	Stress at break (MPa)	Elongation at break (%)
Nafion 115	28 ± 2	180 ± 10
UPBIB	33 ± 2	15 ± 5
DPBIB	29 ± 3	14 ± 4

higher than that of Nafion 115. Generally, the stress at break of PBI-type membranes deteriorates abruptly after doping (~92%) with phosphoric acid and the value dwindles to as low as 3.4 MPa, which makes the membranes unsuitable for applications in HT-PEMFC [37]. For the PBIB membrane, however, the decrease in stress at break value is not so high (~12%), which makes it suitable for use in HT-PEMFC membranes. The main aim of this study is to retain the mechanical property of PBI-type membranes as much as possible even after doping. The hyperbranched honeycomb structure of the polymer helps to counteract the serious weakening of the membrane after doping. Another reason for the reduced weakening of the PBIB membrane after doping is the lower uptake of phosphoric acid. The elongation at break of the UPBIB and the DPBIB films is inferior to that of the Nafion film. This is because of the highly rigid net-structure of the PBIB polymer. Therefore, the flexibility of the PBIB membrane, like other PBI-type membranes, is much lower than the Nafion membrane.

3.6. Proton conductivity

The proton conductivity of the Nafion 115 and DPBIB membranes at 100% relative humidity is presented in Fig. 5. The proton conductivity was measured up to 120 °C, but could not be measured at higher temperatures due to instrument limitations. The proton conductivity of the DPBIB membrane is lower than that of the Nafion 115 membrane up to 120 °C. The proton conductivity of Nafion 115 increases with increasing temperature up to 90 °C, but decreases at 120 °C. On the other hand, the proton conductivity of the DPBIB membrane increases continuously up to 120 °C.

Two models have been proposed for the mechanism of proton transport in a Nafion membrane. According to the Girke cluster channel model, sulfonated side-chains form water-filled clusters through which the proton is transported. If the water content is low, the channels break, which prevents proton transport. The alternative model describes the formation of channels. According to this model, transport channels filled with water and sulfo groups are separated by the hydrophobic polymeric chains. As the water content of the membrane reduces, the channels become narrower, and
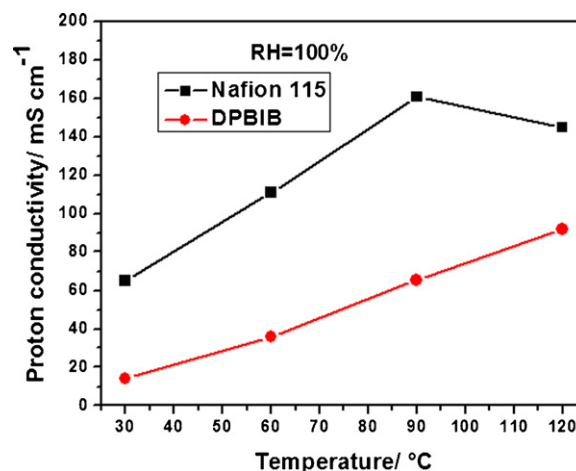

Fig. 5. Proton conductivity as function of temperature for Nafion 115 and DPBIB membranes at 100% relative humidity.
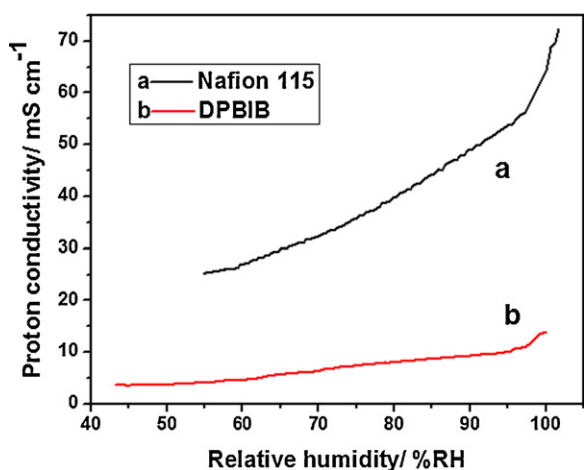
Fig. 6. Effect of humidity on proton conductivity of (a) Nafion 115 and DPBIB membranes at 30 °C.

the proton conductivity decreases concurrently. The two models imply that Nafion membranes can transport protons only in the presence of a sufficient amount of absorbed water. At temperatures above 100 °C, the Nafion membrane loses water and its conductivity decreases sharply [38]. Proton transport in H_3PO_4-doped PBI occurs mainly because of two reasons. One is based on rapid proton-exchange (hopping) between the phosphate and imidazole moieties via hydrogen bonds and the donor (amine)-acceptor (imine) principle, the other explanation is based on self-diffusion of phosphate moieties [11,39]. Hence, with increasing temperature, the proton conductivity of PBI-type membranes is enhanced continuously due to the increase in activation energy for proton transport [38,39]. Therefore, PBI-type membranes can be used for HT-PEMFCs but not Nafion membranes.

The proton conductivity of the DPBIB membrane is much higher than that of PBI [16,40] and sulfonated PBI membranes [33]. This may be due to the highly ordered and compacted honeycomb structure of the PBIB, which ensures easier hoping of protons as the amine and imine groups are expected to be closer in DPBIB compared with that of a linear PBI chain.

The effect of humidity on the proton conductivity of Nafion 115 and DPBIB membranes is shown in Fig. 6. The proton conductivity of the Nafion 115 membrane increases dramatically with increasing relative humidity. By contrast, humidity has only a moderate effect on the proton conductivity of the DPBIB membrane. The cause of this difference in humidity-dependant proton conductivity is the difference in proton transport mechanism, as discussed earlier.

3.7. Fuel cell performance

The performance of Nafion 115 and DPBIB membranes as proton-exchange membranes in an actual fuel cell was examined and compared. Fig. 7 presents the single-cell performance (voltage and power output) as a function of the current density at 70, 100, 130 and 160 °C for the Nafion 115 membrane (under humid conditions) and the DPBIB membrane (with and without humidity). The experiment could not be accomplished above 160 °C because of the limitations of the instrument. For the Nafion 115 membrane, single cell characterization was also carried out without humidity but no power output was observed. This suggests that Nafion cannot be used as a fuel cell membrane under dry conditions. For Nafion 115 under humid conditions, the voltage and power output is decreased continuously with increasing temperature, as shown in Fig. 7(a). This is a normal observation and the reason is concealed in the proton transport mechanism, as discussed above. With increasing
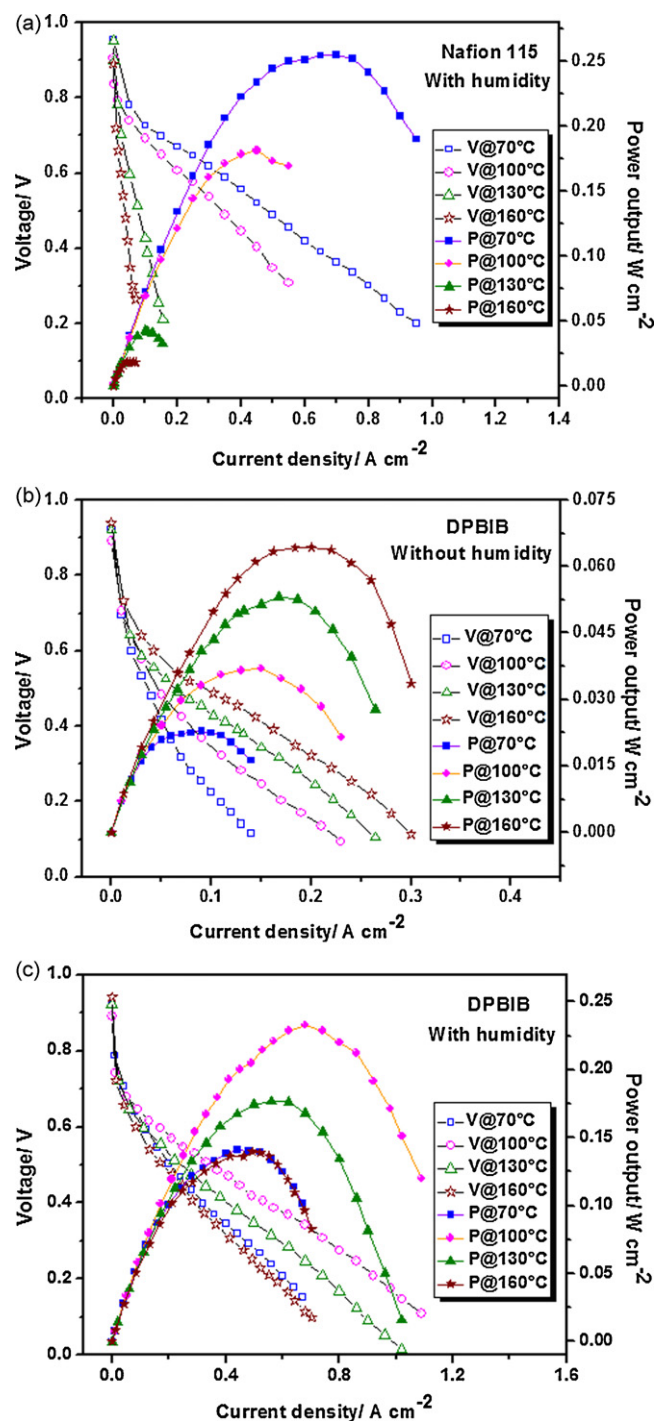

Fig. 7. Single-cell performance (voltage and power output) as function of current density at different temperatures for (a) Nafion 115 membrane under humid conditions, (b) DPBIB membrane without humidity and (c) DPBIB membrane with humidity.

temperature, the water content of the Nafion membrane is reduced, the channels become narrower and the proton conductivity, and hence cell performance, is diminished. Therefore, Nafion is unsuitable as a membrane material for HT-PEMFCs. Fig. 7(b) presents the single-cell performance of the DPBIB membrane under dry conditions. The voltage and power output at different current densities with a DPBIB membrane are ameliorated progressively with increasing temperature. This is attributed to an increase in activation energy for proton transport and to enhanced activity of the platinum catalyst. This suggests that the DPBIB membrane is suit-

able for HT-PEMFCs and the cell can be operated without humidity. If the membrane is operable under dry conditions, a humidifier is not required and the water management issue can be avoided. This will allow a simpler, low cost and portable design of fuel cell system. The maximum power output from the DPBIB membrane under dry conditions is lower than that from the Nafion 115 membrane under humid conditions. Fig. 7(c) presents the single-cell performance of the DPBIB membrane under humid conditions. When the temperature is increased from 70 to 100 °C, the voltage and power output is augmented. When, however, the temperature is further increased from 100 to 130 °C, and then to 160 °C, the performance deteriorates. The power output from the DPBIB membrane at different temperatures is higher under the humid conditions than under the dry conditions. As per the proton transport mechanism in PBI-type membranes, absorbed water is not required; rather, the presence of water may destroy the acid–base complex [38]. By contrast, the proton conductivity of the DPBIB membrane is enhanced with increasing relative humidity, even though the degree of enhancement is less than that for the Nafion 115 membrane (Fig. 6). The improvement in cell performance under humid conditions and the enhancement in proton conductivity with increasing relative humidity suggests that humidity plays some role in the proton transport mechanism in PBI-type membranes. Water molecules may act as connectors between the phosphate and imidazole moieties and enhance amplify the proton-exchange activity (hopping) between them. Water molecules may also act as a lubricant for the phosphate moieties and enhance their self-diffusion. The sulfonic acid groups present in DPBIB might also form water channels and follow the proton transport mechanism as discussed earlier for Nafion membranes. As a result, the proton conductivity and cell performance of DPBIB membrane is dependent to some extent on the relative humidity. When temperature is increased from 70 to 100 °C under humid conditions for the DPBIB membrane, the activation energy for proton transport and activity of the catalyst is increased and hence cell performance is also augmented (Fig. 7c). However, when the temperature is further increased from 100 to 130 °C, and then 160 °C, water is evaporated concurrently. This may increase the gap between the phosphate and imidazole moieties, thereby reducing the efficiency of proton-exchange (hopping) between them and/or abate the lubrication effect that, in turn, suppresses the self-diffusion of the phosphate moieties.

The maximum power output with the DPBIB membrane is comparable with that of the Nafion 115 membrane, when both are under humid conditions.

4. Conclusions

Hyperbranched poly(benzimidazole-co-benzene) (PBIB) with a honeycomb structure has been synthesized by condensation polymerization of trimesic acid (TMA) and 3,3′-diaminobenzidine (DAB), and characterized for use in high-temperature proton-exchange membrane fuel cells (HT-PEMFCs). The hyperbranched honeycomb structure is introduced in order to improve the mechanical strength of the doped membrane. It is difficult to form a UPBIB film from PBIB powder and to dope it with a high amount of phosphoric acid as the polymer is highly ordered and rigid.

The PBIB membrane is thermally stable up to 250 °C. The stress at break of the phosphoric acid doped PBIB (DPBIB) membrane (29 ± 3 MPa) is comparable with that of Nafion (28 ± 2 MPa) and much better than that of phosphoric acid doped PBI-type membranes. On the other hand, the flexibility of the PBIB films, like other PBI-type membranes, is inferior to that of Nafion 115. The DPBIB membrane exhibits lower proton conductivity compared with that of the Nafion 115 membrane. The proton conductivity of the DPBIB membrane is much higher than that of PBI-type mem-

branes, as reported elsewhere. The proton conductivity of Nafion 115 is strongly dependant on relative humidity, whereas humidity has only a moderate effect on the proton conductivity of DPBIB. The Nafion 115 membrane cannot operate in a fuel cell in the absence of humidity, whereas the DPBIB membrane gives good performance.

The performance of a fuel cell with a Nafion 115 membrane under humid conditions deteriorates gradually with increasing cell temperature, whereas, the performance of a cell with a DPBIB membrane under dry conditions is improved progressively with increasing cell temperature. For the DPBIB membrane under humid conditions, the voltage and power output is enhanced with increasing temperature from 70 to 100 °C, but the performance deteriorates markedly when the temperature is increased further from 100 to 130 °C, and then to 160 °C.

The performance of the DPBIB membrane in a fuel cell is much better under humid conditions than under dry conditions. The maximum power output from the DPBIB membrane under dry conditions is lower than that from a Nafion 115 membrane under humid conditions but the output is comparable when both are operated under humid conditions. The difference in the temperature and humidity-dependant proton conductivity and the fuel cell performance between the Nafion 115 and PBIB membranes is attributed to a difference in their proton transporting mechanism. The DPBIB membrane is found to be suitable for application in HT-PEMFCs, whereas the Nafion membrane is unsuitable.

References

[1] B. Viswanathan, M.A. Scibioh, Fuel Cell Principles and Application, CRC press Taylor & Fransis Group, New York, 2007, pp. 272–321.
[2] B.C.H. Steele, A. Heinzel, Nature 414 (2001) 345–352.
[3] K. Sopian, W.R.W. Daud, Renew. Energ. 31 (2006) 719–727.
[4] C. Iojoiu, F. Chabert, M. Marechal, N.El. Kissi, J. Guindet, J.Y. Sanchez, J. Power Sources 153 (2006) 198–209.
[5] J. Jagur-Grodzinski, Polym. Adv. Technol. 18 (2007) 785–799.
[6] J. Zhang, Z. Xie, J. Zhang, Y. Tang, C. Song, T. Navessin, Z. Shi, D. Song, H. Wang, D.P. Wilkinson, Z.S. Liu, S. Holdcroft, J. Power Sources 160 (2006) 872–891.
[7] Q. Li, R. He, J.O. Jensen, N.J. Bjerrum, Chem. Mater. 15 (2003) 4896–4915.
[8] B. Smitha, S. Sridhar, A.A. Khan, J. Membr. Sci. 259 (2005) 10–26.
[9] K.D. Kreuer, J. Membr. Sci. 185 (2001) 29–39.
[10] J.S. Wainright, J.T. Wang, D. Weng, R.F. Savinell, M. Litt, J. Electrochem. Soc. 142 (1995) L121–L123.
[11] Y.L. Ma, J.S. Wainright, M.H. Litt, R.F. Sanivel, J. Electrochem. Soc. 151 (2004) A8–A16.
[12] R. He, Q. Li, G. Xiao, N.J. Bjerrum, J. Membr. Sci. 226 (2003) 169–184.
[13] Z.G. Shao, P. Joghee, I.M. Hsing, J. Membr. Sci. 229 (2004) 43–51.
[14] Q. Li, H.A. Hjuler, N.J. Bjerrum, J. Appl. Electrochem. 31 (2001) 773–779.
[15] M.F.H. Schuster, W.H. Meyer, M. Schuster, K.D. Kreuer, Chem. Mater. 16 (2004) 329–337.
[16] J. Lobato, P. Canizares, M.A. Rodrigo, J.J. Linares, J.A. Aguilar, J. Membr. Sci. 306 (2007) 47–55.
[17] J. Kerres, D. Xing, F. Schonberger, J. Polym. Sci. Polym. Phys. 44 (2006) 2311–2326.
[18] J.K. Gillham, Science 139 (1963) 494–495.
[19] J.S. Young, G.S. Long, S. Gregory, B.F. Espinoza, US Patent 6,997,971.
[20] K.Y. Wang, Y.C. Xiao, T.S. Chung, Chem. Eng. Sci. 61 (2006) 5807–5817.
[21] Q. Li, C. Pan, J.O. Jensen, Pernille Noye, J. Niels, Bjerrum, Chem. Mater. 19 (2007) 350–352.
[22] P. Noye, Q. Li, C. Pan, N. Bjerrum, Polym. Adv. Technol. 19 (2008) 1270–1275.
[23] J. Lobato, P. Canizares, M.A. Rodrigo, J.J. Linares, G. Manjavacas, J. Membr. Sci. 280 (2006) 351–362.
[24] J. Peron, E. Ruiz, D.J. Jones, J. Roziere, J Membr. Sci. 314 (2008) 247–256.
[25] G. Gauglitz, T. Vo-Dinh, Handbook of Spectroscopy, 1, WILEY-VCH Verlag GmbH & Co. KGaA, Weinheim, 2003, pp. 100–105.
[26] J.R. Dyer, Applications of Absorption Spectroscopy of Organic Compounds, Eastern Economy Edition, Prentice Hall of India Private Limited, New Delhi, India, 2002, pp. 33–38.
[27] S. Qing, W. Huang, D. Yan, Eur. Polym. J. 41 (2005) 1589–1595.

[28] S. Bhadra, D. Khastgir, Polym. Degrad. Stab. 93 (2008) 1094–1099.
[29] S. Bhadra, N.K. Singha, D. Khastgir, J. Appl. Polym. Sci. 104 (2007) 1900–1904.
[30] M.J. Ariza, D.J. Jones, J. Roziere, Desalination 147 (2002) 183–189.
[31] J. Pang, H. Zhang, X. Li, Z. Jiang, N. Wholly, Macromolecules 40 (2007) 9435–9442.
[32] B.H. Aristizabal, C.M. Correa, A.I. Serykh, C.E. Hetrick, M.D. Amiridis, J. Catal. 258 (2008) 95–102.
[33] S. Qing, W. Huang, D. Yan, React. Funct. Polym. 66 (2006) 219–227.
[34] H. Xu, K. Chen, X. Guo, J. Fang, J. Yin, Polymer 48 (2007) 5556–5564.
[35] S. Bhadra, N.K. Singha, D. Khastgir, J. Appl. Polym. Sci. 107 (2008) 2486–2493.
[36] H. Xu, K. Chen, X. Guo, J. Fang, J. Yin, J. Membr. Sci. 288 (2007) 255–260.
[37] R. He, Q. Che, B. Sun, Fibers Polym. 9 (2008) 679–684.
[38] Y.A. Dobrovolskii, E.V. Volkov, A.V. Pisareva, Y.A. Fedotov, D.Y. Likhachev, A.L. Rusanov, Khimicheskii Zhurnal 50 (2007) 95–104.
[39] H. Pu, W.H. Meyer, G. Wegner, J. Polym. Sci. Polym. Phys. 40 (2002) 663–669.
[40] J.A. Asensio, S. Borros, P. Gomez-Romero, J. Electrochem. Soc. 151 (2004) A304–A310.